ROCKY MOUNTAIN
JOURNAL OF MATHEMATICS
Volume 38, Number 5, 2008

DYNAMIC BEHAVIORS OF A SINGLE-SPECIES POPULATION MODEL WITH BIRTH PULSES IN A POLLUTED ENVIRONMENT

FENGMEI TAO AND BING LIU

In this paper, we investigate the dynamics of a single-species model with birth pulses, pulse harvesting and pulse toxicant input in a polluted environment. Using the discrete dynamical system determined by the stroboscopic map, we obtain an exact 1-period solution of system whose birth function is the Ricker function or Beverton-Holt function, and obtain the threshold conditions for their stability. Further, we show the effects of the time of pulse harvesting and pulse toxicant input on the maximum annual-sustainable yield. Our results show that the best time of harvesting is immediately after the birth pulses, and the maximum annual-sustainable yield is not significantly affected by the time of toxicant input. Numerical simulation results also show that birth pulses, pulse harvesting and pulse toxicant input make the single-species model in the polluted environment we consider more complex, and the systems are dominated by periodic and chaotic solutions.

1. Introduction. Due to rapid technological advances and significant increases in the human population during the past half century, the amount of the world's fish has been deeply decreased. About three quarters of the world's marine fisheries are either fully exploited or over-exploited. Such heavy use of these resources means that our main task is to strengthen global efforts to ensure the effective and sustainable use of marine resources and the sound management of the ecosystem. Therefore, it is very realistic for decision-makers to plan practicable schemes which sustain fisheries at a good level of productivity and meet economic goals. Economic and biological aspects of renewable resources management have been considered by Clark [**6**] and other authors [**2,**

Keywords and phrases. Birth pulse, pulse harvesting, pulse toxicant input, bifurcation, chaos.

This work is supported by National Natural Science Foundation of China (10671100), by China Postdoctoral Science Foundation 2005037253, by Science and Research Project Foundation of Liaoning Province Education Department and by Science and Technology Project of Anshan.

Received by the editors on August 20, 2007, and in revised form on January 3, 2008.

DOI:10.1216/RMJ-2008-38-5-1663

32–34]. However, most existing theories on harvest strategies largely ignore the effects of seasonality and environmental pollution. In 2005, Xu et al. [**34**] investigated harvesting in seasonal environments and focused on maximum annual yield (MAY) and population persistence under five commonly used harvest strategies. They concluded that pulse harvesting is the best amongst all the strategies that they had explored with much larger MAY and mean population size but smaller population variability at MAY. Also they obtained that harvest timing was of large importance to annual yield and population persistence for pulse harvesting. Harvesting too late may overexploit a population risking extinction with much smaller MAY as well.

Environmental pollution by various industries is one of the most important of present day socio-ecological problems. Uncontrolled contribution of pollutant to the environment has led many species to extinction and several others are on the verge of extinction. Such environmental uncertainty also affects the incentive to harvest a resource. The nature of optimal exploitation and its effects on the dynamics of biological populations when the growth process of a specie is subject to random environmental shocks are not very well understood. In recent years some investigations have been conducted to study the effect of toxicant emitted into the environment from industrial and household sources on biological species ([**9, 11, 14, 24**]) by using mathematical models, but most of the previous models have invariably assumed that the exogenous input of toxicant is continuous; however, it is often the case that toxicant is emitted in regular pulses. One example is the use of pesticides. Pesticides are useful tools in agriculture and forestry because they quickly kill a significant portion of a pest population and they sometimes provide the only feasible method for preventing economic loss. Pesticides can be sprayed instantaneously and regularly. Another example is the pollution by heavy metals. Most of heavy metal pollution of river and consequently of soil is caused by artificial industry. When the pollutants of heavy metal drain into the environment, they affect human population and other biological species seriously, such as pulse copper pollution ([**17, 18**]). Therefore, the continuous input of toxicant is then removed from the model and replaced with an impulsive perturbation. In this case, although the input of toxicant is transient, the effect of toxicant on the species is continuous. So in this paper, considering the results in [**34**], we will study an optimal

pulse harvesting problem of a single species in a polluted environment with pulse toxicant input and see how the pulse harvesting and pulse toxicant input affect population persistence and the volume of mature fish stock in a polluted environment. How do the pulse harvesting and pulse toxicant input affect the maximum annual-sustainable yield? Can we obtain similar results to those of [**34**]?

In most models of population dynamics, an increase in population due to birth is assumed to be time dependent, but many species reproduce only during a short period of the year. In between these pulses of growth, mortality takes its toll and the population decreases. Basing on the single-species model with continuous harvesting policy in a polluted environment and integrating the ideas of pulse harvesting, pulse toxicant input and birth pulses mentioned above, we suggest an impulsive equation, see [**3, 21**], to model the processes of birth pulses and pulse harvesting at different fixed times in a polluted environment and investigate the dynamics of the system. We want to know the effects of pulse harvesting, pulse toxicant input and birth pulses on the dynamics of the system and compare our results with those in [**34**]. To our knowledge, there have been no results on this problem in the literature. Impulsive equations are found in almost every domain of applied science and has been studied in many investigations [**1, 12, 22–26, 28, 30, 31, 32**].

The organization of this paper is as follows. In the next section, we formulate a single-species population model with pulse harvesting, pulse toxicant input and birth pulses in a polluted environment by using impulsive equation. In Section 3, we investigate the dynamics of such a system by using the stroboscopic map. In Section 4, we focus our attention on the relationships between the differential dynamical system with birth pulses and the discrete dynamical system determined by the corresponding stroboscopic map. In Section 5, numerical simulations show how the dynamics are affected by changes in birth rate, the harvesting effort and toxicant input amount, and whether chaos will occur in such a system. In Section 6, we study the effects of pulse harvesting time and pulse toxicant input on the maximum annual-sustainable yield. In the last section, we conclude our results.

2. Model formulation. In the absence of a polluted environment, we assume that the size of single species changes according to the

following population growth equation

$$\dot{x}(t) = B(x)x(t) - dx(t), \tag{2.1}$$

where $d > 0$ is the death rate constant and $B(x)x$ is a birth rate function with $B(x)$ satisfying the following basic assumptions for $N \in (0, \infty)$:

(A_1) $B(x) > 0$;

(A_2) $B(x)$ is continuously differentiable with $B'(x) < 0$;

(A_3) $B(0^+) > d > B(\infty)$.

Note that (A_2) and (A_3) imply that $B^{-1}(x)$ exists for $x \in (B(\infty), B(0^+))$, and (A_3) gives the existence of a carrying capacity K such that $B(x) > d$ for $x < K$ and $B(x) < d$ for $x > K$. Under these assumptions, nontrivial solutions of (2.1) approach $B^{-1}(d)$ as $t \to \infty$.

Examples of birth functions $B(x)$ found in the biological literature that satisfy (A_1)–(A_3) are:

(B_1) $B_1(x) = be^{-x}$, with $b > d$;

(B_2) $B_2(x) = b/(q + x^n)$, with $b, q, n > 0$ and $b/q > d$.

(B_3) $B_3(x) = (A/x) + c$ with $A > 0$, $d > c > 0$.

Functions B_1 and B_2 with $n = 1$ are used in fisheries and are known as the Ricker function and Beverton-Holt function, respectively. Function $B_3(x)x$ represents a constant immigration rate A together with a linear birth term cx.

For the population model (2.1), it can be postulated that the size of the population is affected by the input of toxicant, and the presence of toxicant in the environment decreases the growth rate of species. These lead to the following single population model with toxicant effects in

the polluted environment:

$$\text{(2.2)}\qquad \begin{cases} \dfrac{dx(t)}{dt} = x(t)(B(x) - rc(t) - d), \\ \dfrac{dc(t)}{dt} = kf(t) - g_1c(t) - g_2c(t), \\ \dfrac{df(t)}{dt} = -k_1f(t)x(t) - hf(t) + k_2c(t)x(t) + u(t), \end{cases}$$

where $x(t)$ is the density of the species at time t; $c(t)$ is the concentration of the toxicant in the organism at time t; $f(t)$ is the concentration of the toxicant in the environment at time t; $B(x)x$ is a birth rate function satisfying the assumptions (A_1)–(A_3); The meanings of other parameters are the same as those of model (2.1) in [**24**].

In this paper, we assume that the capacity of the environment is so large that the change of toxicant in the environment that comes from uptake and egestion by the organisms can be ignored ($k_1 = 0$, $k_2 = 0$) and the toxicant input is constant ($u(t) = u$). For convenience of computation, let $g = g_1 + g_2$.

Now, considering the above assumptions and the continuous harvesting policy of the population, we construct the following system:

$$\text{(2.3)}\qquad \begin{cases} \dfrac{dx(t)}{dt} = x(t)(B(x) - rc(t) - d - E), \\ \dfrac{dc(t)}{dt} = kf(t) - gc(t), \\ \dfrac{df(t)}{dt} = u - hf(t), \end{cases}$$

where E denotes the harvesting effort.

Model (2.3) has invariably assumed that the population is born throughout the year, whereas it is often the case that births are seasonal or occur in regular pulses. Many large mammal and fish population exhibit what Caughley [**6**] termed a "birth pulse" growth pattern. That is, reproduction takes place in a relatively short period each year. In this paper, we take pulse harvesting policy and assume the time we take to harvest is fixed every year. Also we remove the continuous input of toxicant in model (2.3) and consider pulse toxicant input at fixed moment in a polluted closed environment. Now, based on

the impulsive differential equations, we will develop system (2.3) by introducing periodic birth pulses, pulse harvesting and pulse toxicant input at different fixed time. That is, we consider the following system:

$$
\begin{cases}
\left.\begin{aligned} \frac{dx(t)}{dt} &= -rc(t)x(t) - dx(t), \\ \frac{dc(t)}{dt} &= kf(t) - gc(t), \\ \frac{df(t)}{dt} &= -hf(t), \end{aligned}\right\} \begin{array}{l} t \neq m+1, \\ t \neq m+T_1, \\ t \neq m+T_2, \end{array} \\
\left.\begin{aligned} x(t^+) &= x(t), \\ c(t^+) &= c(t), \\ f(t^+) &= f(t) + \mu, \end{aligned}\right\} \quad t = m + T_1, \\
\left.\begin{aligned} x(t^+) &= (1-E)x(t), \\ c(t^+) &= c(t), \\ f(t^+) &= f(t), \end{aligned}\right\} \quad t = m + T_2, \\
\left.\begin{aligned} x(t^+) &= x(t) + B(x(t))x(t), \\ c(t^+) &= c(t), \\ f(t^+) &= f(t), \end{aligned}\right\} \begin{array}{c} t = m+1, \\ m \in Z_0 = \{0, 1, 2, \dots\}, \end{array}
\end{cases} \tag{2.4}
$$

where the meanings of parameters r, d, k, g, h and E are the same as model (2.3); $x(t^+)$ is the quantity of population after the birth pulse, $x(t^+) = \lim_{t \to t^+} x(t)$, $c(t^+) = \lim_{t \to t^+} c(t)$, $f(t^+) = \lim_{t \to t^+} f(t)$. For convenience, here we assume that the toxicant input has only one and the population $x(t)$ can reproduce only once in each year. $0 \leq T_1 \leq 1$ represents the time of pulse toxicant input in each year; $0 \leq T_2 \leq 1$ represents the time of pulse harvesting in each year; $\mu > 0$ represents toxicant input amount at time $m + T_1$, $0 < E < 1$ represents pulse harvesting effort at $t = m + T_2$, $m \in Z_0$. In the following section, we will investigate the dynamics of system (2.4).

3. Dynamical behaviors of system (2.4).

3.1 Stroboscopic maps of system (2.4) with Ricker function and Beverton-Holt function. We can easily obtain the analytical

solution of system (2.4) at the interval $[m, m+1)$. Let

$$
\begin{aligned}
F_1 &= \frac{krf_m}{g-h}\left(\frac{1}{g}(1-e^{-g(t-m)})-\frac{1}{h}(1-e^{-h(t-m)})\right)\\
&\quad -\frac{r}{g}c_m(1-e^{-g(t-m)}),\\
F_2 &= \frac{k\mu r}{g-h}\left(\frac{1}{g}(1-e^{-g(t-(m+T_1))})-\frac{1}{h}(1-e^{-h(t-(m+T_1))})\right),\\
F_3 &= \frac{k\mu}{g-h}(e^{-h(t-(m+T_1))}-e^{-g(t-(m+T_1))}),
\end{aligned}
$$

if $0 < T_1 < T_2 < 1$. Then

(3.1)

$$
\begin{cases}
\left.\begin{aligned}
x(t) &= x_m e^{F_1-d(t-m)}\\
c(t) &= \frac{kf_m}{g-h}(e^{-h(t-m)}-e^{-g(t-m)})\\
&\qquad + c_m e^{-g(t-m)}\\
f(t) &= f_m e^{-h(t-m)}
\end{aligned}\right\} & m \le t < m+T_1\\
\left.\begin{aligned}
x(t) &= x_m e^{F_1+F_2-d(t-m)}\\
c(t) &= \frac{kf_m}{g-h}(e^{-h(t-m)}-e^{-g(t-m)})\\
&\qquad + c_m e^{-g(t-m)}+F_3\\
f(t) &= f_m e^{-h(t-m)}+\mu e^{-h(t-(m+T_1))}
\end{aligned}\right\} & \begin{matrix} m+T_1\\ \le t < m+T_2 \end{matrix}\\
\left.\begin{aligned}
x(t) &= (1-E)x_m e^{F_1+F_2-d(t-m)}\\
c(t) &= \frac{kf_m}{g-h}(e^{-h(t-m)}-e^{-g(t-m)})\\
&\qquad + c_m e^{-g(t-m)}+F_3\\
f(t) &= f_m e^{-h(t-m)}+\mu e^{-h(t-(m+T_1))}
\end{aligned}\right\} & \begin{matrix} m+T_2\\ \le t < m+1; \end{matrix}
\end{cases}
$$

if $0 < T_2 < T_1 < 1$. Then

(3.2)
$$\begin{cases} \left.\begin{aligned} x(t) &= x_m e^{F_1 - d(t-m)} \\ c(t) &= \frac{kf_m}{g-h}(e^{-h(t-m)} - e^{-g(t-m)}) \\ &\quad + c_m e^{-g(t-m)} \\ f(t) &= f_m e^{-h(t-m)} \end{aligned}\right\} & m \le t \\ & < m + T_2, \\ \left.\begin{aligned} x(t) &= (1-E)x_m e^{F_1 - d(t-m)} \\ c(t) &= \frac{kf_m}{g-h}(e^{-h(t-m)} - e^{-g(t-m)}) \\ &\quad + c_m e^{-g(t-m)} \\ f(t) &= f_m e^{-h(t-m)} \end{aligned}\right\} & m + T_2 \\ & \le t < m + T_1, \\ \left.\begin{aligned} x(t) &= (1-E)x_m e^{F_1 + F_2 - d(t-m)} \\ c(t) &= \frac{kf_m}{g-h}(e^{-h(t-m)} - e^{-g(t-m)}) \\ &\quad + c_m e^{-g(t-m)} + F_3 \\ f(t) &= f_m e^{-h(t-m)} + \mu e^{-h(t-(m+T_1))} \end{aligned}\right\} & m + T_1 \le \\ & t < m + 1, \end{cases}$$

where x_m, c_m and f_m denote the densities of the population, the concentration of the toxicant in the organism, and the concentration of the toxicant in the environment at time m, respectively. For the Ricker function, i.e., $B(x) = be^{-x}$, equation (3.1) (or (3.2)) holds on the interval $[m, m+1)$. After each successive birth pulse, more of population is added, yielding

(3.3)
$$\begin{cases} x_{m+1} = (1 + be^{-A(m)x_m})A(m)x_m, \\ c_{m+1} = (kf_m/g - h)(e^{-h} - e^{-g}) + (k\mu/g - h)(e^{-h(1-T_1)} - e^{-g(1-T_1)}) \\ \qquad\qquad + c_m e^{-g}, \\ f_{m+1} = f_m e^{-h} + \mu e^{-h(1-T_1)}. \end{cases}$$

where

$$\begin{aligned} A(m) = (1-E)e^{(kr)/(g-h)f_m((1/g)(1-e^{-g})-(1/h)(1-e^{-h}))} \\ + e^{(k\mu r)/(g-h)((1/g)(1-e^{-g(1-T_1)})-(1/h)(1-e^{-h(1-T_1)}))} \\ - e^{(r/g)c_m(1-e^{-g})-d}. \end{aligned}$$

Similarly, for the Beverton-Holt function, i.e., $B(N) = b/(q+x^n)$, we have the following stroboscopic map of system (3.2):

$$\text{(3.4)} \quad \begin{cases} x_{m+1} = (1+(b/q+(A(m)x_m)^n))A(m)x_m, \\ c_{m+1} = (kf_m)/(g-h)(e^{-h}-e^{-g}) \\ \qquad\quad +(k\mu)/(g-h)(e^{-h(1-T_1)}-e^{-g(1-T_1)})+c_m e^{-g}, \\ f_{m+1} = f_m e^{-h} + \mu e^{-h(1-T_1)}. \end{cases}$$

Equations (3.3) and (3.4) are difference equations. They describe the density of the population, the concentration of the toxicant in the organism, and the concentration of the toxicant in the environment at $t = m+1$ in terms of values at $t = m$. We are, in other words, stroboscopically sampling at its pulsing period $t = m+1$, $m \in Z^+$. The dynamics of system (3.3) and system (3.4), coupled with system (3.1) (or 3.2)), determine the dynamical behavior of system (2.4) for the Ricker function and for the Beverton-Holt function, respectively. Thus, in the following we will focus our attention on system (3.3) and system (3.4), and investigate the various dynamical behaviors.

The dynamics of these nonlinear models can be studied as a function of any of the parameters. Here we will focus on b for the Ricker function and the Beverton-Holt function, and expound the changes in the qualitative dynamics of the models (3.3) and (3.4) as b varies.

3.2. Stability of nonnegative equilibria of system (3.3) and system (3.4). The system (3.3) (or equation (3.4)) exists as a trivial equilibrium $E_0(0, c^*, f^*)$, where $c^* = (k\mu(e^{-h(1-T_1)} - e^{-g(1-T_1)} + e^{-(h+g)}(e^{gT_1} - e^{hT_1})))/((g-h)(1-e^{-h})(1-e^{-g}))$, $f^* = (\mu e^{-h(1-T_1)})/(1-e^{-h})$ and a unique positive equilibrium $E^* = (x^*, c^*, f^*)$ if $R_0 > 1$, which are listed in Table 1.

In the neighborhood of E_0 (E^*), the dynamics of equations (3.3) and (3.4) are controlled by the linearization,

$$\text{(3.5)} \qquad Y_{m+1} = CY_m$$

TABLE 1. Nontrivial equilibria of the two models with birth pulses.

Function	Equilibrium	$R_0 = R_0^R$ (or R_0^B)
Ricker	$x^* = 1/(1-E)e^{d+(k\mu r)/(gh)} \ln R_0^R$ $c^* = (k\mu(e^{-h(1-T_1)} - e^{-g(1-T_1)}$ $+e^{-(h+g)}(e^{gT_1} - e^{hT_1})))/((g-h)(1-e^{-h})(1-e^{-g}))$ $f^* = (\mu e^{-h(1-T_1)})/(1-e^{-h})$	$R_0^R = b((1/1-E)$ $e^{d+(k\mu r)/(gh)} - 1)^{-1}$
Beverton-Holt	$x^* = (1/1-E)e^{d+(k\mu r)/(gh)} \sqrt[n]{q(R_0^B - 1)}$ $c^* = (k\mu(e^{-h(1-T_1)} - e^{-g(1-T_1)}$ $+e^{-(h+g)}(e^{gT_1} - e^{hT_1})))/((g-h)(1-e^{-h})(1-e^{-g}))$ $f^* = (\mu e^{-h(1-T_1)})/(1-e^{-h})$	$R_0^B = (b/q)((1/1-E)$ $e^{d+(k\mu r)/(gh)} - 1)^{-1}$

with C equal to the linearization counterpart of equation (3.3) or (3.4) and $Y = (x, c, f)$. E_0 (or E^*) is stable when the absolute values of eigenvalues of C are all less than one.

For the trivial equilibrium $E_0(0, c^*, f^*)$ of equation (3.3),

$$C_{E_0}^R = \begin{pmatrix} (1+b)/\beta & * & * \\ 0 & e^{-g} & (k/g-h)(e^{-h} - e^{-g}) \\ 0 & 0 & e^{-h} \end{pmatrix}$$

where $\beta = (1/1-E)e^{d+(k\mu r)/(gh)} > 1$ and there is no need to calculate the exact form of $(*)$ as they are not required in the analysis that follows.

The eigenvalues of $C_{E_0}^R$ are $\lambda_1 = (1+b)/\beta$, $\lambda_2 = e^{-g} < 1$ and $\lambda_3 = e^{-h} < 1$, if

$$\frac{1+b}{\beta} < 1; \tag{3.6}$$

then E_0 is locally asymptotically stable. In terms of model parameters, and after a bit of rearranging, for equation (3.3), inequality (3.6) reads

$$b < \beta - 1 \equiv b_0^R. \tag{3.7}$$

Similarly, for the trivial equilibrium $E_0(0, c^*, f^*)$ of equation (3.4),

$$C_{E_0}^B = \begin{pmatrix} (1/\beta)(1+(b/q)) & * & * \\ 0 & e^{-g} & (k/g-h)(e^{-h} - e^{-g}) \\ 0 & 0 & e^{-h} \end{pmatrix}.$$

So if

$$b < q(\beta - 1) \equiv b_0^B, \tag{3.8}$$

then E_0 is locally asymptotically stable.

Thus, if inequality (3.7) (or (3.8)) holds true, $E_0(0, c^*, f^*)$ is stable. For this range of b, the population will be extinct. Otherwise, $E_0(0, c^*, f^*)$ is unstable and a small population will be increased from $E_0 = (0, c^*, f^*)$.

For the difference equations (3.3) and (3.4), we can also define the intrinsic net reproductive number R_0 (the average number of offspring which an individual produces over the course of its lifetime). For equation (3.3), R_0 is given by

$$R_0^R = b(\beta - 1)^{-1}.$$

For equation (3.4), R_0 is given by

$$R_0^B = \frac{b}{q}(\beta - 1)^{-1}.$$

Inequality (3.7) ((3.8)) can be rewritten as $R_0^R < 1$ ($R_0^B < 1$). That is, if on average, individuals do not replace themselves before they die, then the population is doomed.

Note that when $b = b_0$, i.e., $R_0^R = R_0^B = 1$, then $E^* = (0, c^*, f^*) = E_0$. Thus, as b increases through b_0, E^* passes through the equilibrium at E_0 and exchanges stability with it in a transcritical bifurcation.

For the linearization C of equation (3.3) about this positive equilibrium E^*,

$$C_{E_*}^R = \begin{pmatrix} 1 - (1 - (1/\beta)) \ln(R_0^R) & * & * \\ 0 & e^{-g} & (k/g - h)(e^{-h} - e^{-g}) \\ 0 & 0 & e^{-h} \end{pmatrix}.$$

There is no need to calculate the exact form of $(*)$ as it is not required in the analysis that follows.

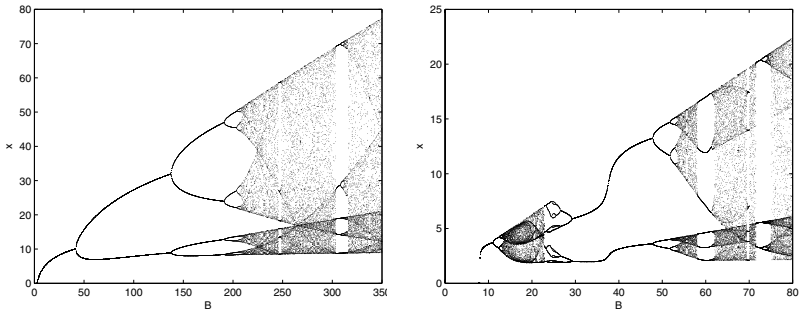

(a) (b)

FIGURE 1. Bifurcation diagrams of equations (3.3) and (3.4) for the population $x(t)$. This shows the effect of parameter b on dynamical behavior. Parameter values are $k = 1$, $g = 1.2$, $h = 2$, $r = 1$, $d = 0.4$, $\mu = 0.5$, $T = 0.25$, $E = 0.5$, $q = 3$, $n = 10$. (a) Ricker function, $b \in [0, 350]$. (b) Beverton-Holt function, $b \in [0, 80]$.

The eigenvalues of $C^R_{E_*}$ are $\lambda'_1 = 1 - (1 - (1/\beta)) \ln R^R_0 < 1$, $0 < \lambda'_2 = e^{-g} < 1$, $0 < \lambda'_3 = e^{-h} < 1$, if

$$1 - \left(1 - \frac{1}{\beta}\right) \ln R^R_0 > -1; \tag{3.9}$$

then E^* is locally asymptotically stable.

Similarly, the linearization C of equation (3.4) about this positive equilibrium E^*,

$$C^B_{E_*} = \begin{pmatrix} 1 - n(1 - (1/\beta))(1 - (1/R^B_0)) & * & * \\ 0 & e^{-g} & (k/g - h)(e^{-h} - e^{-g}) \\ 0 & 0 & e^{-h} \end{pmatrix}.$$

If

$$1 - n\left(1 - \frac{1}{\beta}\right)\left(1 - \frac{1}{R^B_0}\right) > -1, \tag{3.10}$$

then E^* is locally asymptotically stable.

The stability of E^* is lost in only one way as b increases. Condition (3.9) or (3.10) is violated for $b > b_c$. The critical values are listed in Table 2 for each model. A flip bifurcation occurs and the equilibrium loses stability to a stable two-cycle, see Figure 1.

TABLE 2. Critical value b_c of the parameter b for each model. b must be less than b_c for stability.

Function	b_c	Interval of stability	Type of bifurcation
Ricker	$b_c^R = (\beta-1)e^{(2\beta)/(\beta-1)}$	$b_0^R < b < b_c^R$	Flip bifurcation
Beverton-Holt	$b_c^B = \dfrac{c(\beta-1)}{1-(2/n(1-(1/\beta)))}$	$b_0^B < b < b_c^B$	Flip bifurcation

4. The relationships between model (2.4) and model (3.3) (or (3.4)). In Section 3, we present the dynamics of system (2.4) using the stroboscopic map. This is a special case of the Poincaré map for a periodically forced system or periodically pulsed system; the system trajectory is not recorded continuously in time but once every harvesting period. Long-term solutions of system (2.4) will then appear as follows.

(i) Fixed point of the stroboscopic map (corresponding to 1-period solution having the same period as the birth pulse term).

(ii) Periodic points of the stroboscopic map, of period k (corresponding to k-period solutions, often called subharmonic periodic solutions or subharmonic period k's).

(iii) Invariant circles (corresponding to quasi-periodic solutions, tori T^2 for the original system of impulsive differential equations).

(iv) Chaotic (strange) attractors.

In the following, we show that the solutions of system (3.3) behave like the above three cases (i), (ii) and (iv).

For $b < b_0$, the equilibrium $E_0(0, c^*, f^*)$ is stable. For this range of b, trajectories of model (2.4) approach the origin.

For $b_0 < b < b_c$, the equilibrium E^* is stable. For this range of b, trajectories of models (3.3) and (3.4) approach the 1-period solution $(\tilde{x}(t), \tilde{c}(t), \tilde{f}(t))$. If $0 < T_1 < T_2 < 1$,

(4.1)

$$\begin{cases} \tilde{x}(t) = \begin{cases} x^* e^{F_1^* - d(t-m)}, & m \le t < m + T_1, \\ x^* e^{F_1 + F_2 - d(t-m)}, & m + T_1 \le t < m + T_2, \\ (1-E) x^* e^{F_1 + F_2 - d(t-m)}, & m + T_2 \le t < m + 1, \end{cases} \\ \tilde{c}(t) = \begin{cases} \dfrac{kf^*}{g-h}(e^{-h(t-m)} - e^{-g(t-m)}) + c^* e^{-g(t-m)}, & m \le t < m + T_1 \\ \dfrac{kf^*}{g-h}(e^{-h(t-m)} - e^{-g(t-m)}) + c^* e^{-g(t-m)} + F_3^*, & m + T_1 \le t < m + 1, \end{cases} \\ \tilde{f}(t) = \begin{cases} f^* e^{-h(t-m)}, & m \le t < m + T_1, \\ f^* e^{-h(t-m)} + \mu e^{-h(t-(m+T_1))}, & m + T_1 \le t < m + 1, \end{cases} \end{cases}$$

where

$$F_1^* = \frac{krf*}{g-h}\left(\frac{1}{g}(1 - e^{-g(t-m)}) - \frac{1}{h}(1 - e^{-h(t-m)})\right) - \frac{r}{g}c^*(1 - e^{-g(t-m)}),$$

$$F_2^* = \frac{k\mu r}{g-h}\left(\frac{1}{g}(1 - e^{-g(t-(m+T_1))}) - \frac{1}{h}(1 - e^{-h(t-(m+T_1))})\right),$$

$$F_3^* = \frac{k\mu}{g-h}(e^{-h(t-(m+T_1))} - e^{-g(t-(m+T_1))}).$$

If $0 < T_2 < T_1 < 1$, then

(4.2)

$$\begin{cases} \tilde{x}(t) = \begin{cases} x^* e^{F_1 - d(t-m)}, & m \le t < m + T_1, \\ (1-E) x^* e^{F_1^* - d(t-m)}, & m + T_1 \le t < m + T_2, \\ (1-E) x^* e^{F_1^* + F_2^* - d(t-m)}, & m + T_2 \le t < m + 1, \end{cases} \\ \tilde{c}(t) = \begin{cases} \dfrac{kf^*}{g-h}(e^{-h(t-m)} - e^{-g(t-m)}) + c^* e^{-g(t-m)}, & m \le t < m + T_1, \\ \dfrac{kf^*}{g-h}(e^{-h(t-m)} - e^{-g(t-m)}) + c^* e^{-g(t-m)} + F_3^*, & m + T_1 \le t < m + 1, \end{cases} \\ \tilde{f}(t) = \begin{cases} f^* e^{-h(t-m)}, & m \le t < m + T_1, \\ f^* e^{-h(t-m)} + \mu e^{-h(t-(m+T_1))}, & m + T_1 \le t < m + 1, \end{cases} \end{cases}$$

That is, the 1-period solution (4.1) (or(4.2)) of system (2.4) is locally asymptotically stable. Right at $b = b_0$, there is a transcritical

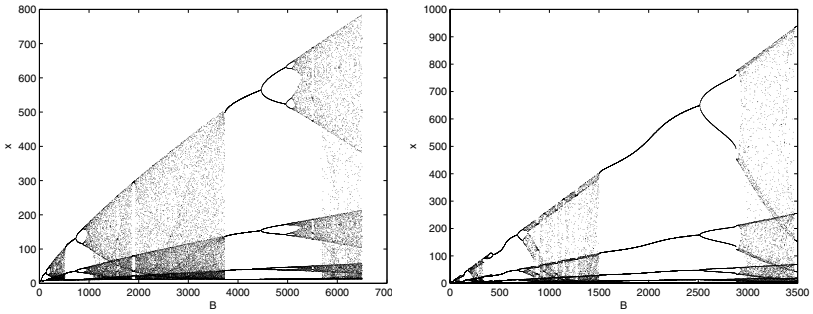

(a) (b)

FIGURE 2. Bifurcation diagrams of equations (3.3) and (3.4) for the population $x(t)$. This shows the effect of parameter b on dynamical behavior. Parameter values are $k = 1$, $g = 1.2$, $h = 2$, $r = 1$, $d = 0.4$, $\mu = 0.5$, $T_1 = 0.25$, $T_2 = 0.5$, $E = 0.5$, $q = 3$, $n = 10$. (a) Ricker function, $b \in [0, 6500]$. (b) Beverton-Holt function, $b \in [0, 3500]$.

bifurcation of periodic solutions. $(0, 0, 0)$ and $(\tilde{x}(t), \tilde{c}(t, \tilde{f}(t))$ pass through each other and exchange stability.

As b increases beyond b_c, it passes through a cascade of period-doubling bifurcations that eventually lead to chaotic dynamics and many other complexities (see Figure 1 and Figure 2). For details, see Section 5.

5. Numerical analysis. Our focus so far has been on the equilibria of systems (3.3) and (3.4), and in particular, on the existence and stability of those equilibria. But, if the parameter is beyond some critical value, the models exhibit a wide variety of dynamical behavior. The dynamics of nonlinear models can be studied as a function of any one of the parameters, and we will focus on parameters b, E and μ.

As b increases beyond b_c, each model passes through a series of period-doubling bifurcations that eventually lead to chaotic dynamics. In Figures 1 and 2, we have displayed typical bifurcation diagrams for each model. For the Ricker function, when $2.67 < b < 41.74$, the 1-period solution of system (2.4) is still stable. When $b > 41.7$, it becomes unstable, and there is a cascade of period doubling bifurcations leading to chaos. This period-doubling route to chaos is the hallmark of the logistic and Ricker maps (see [**27**]) and has been studied by mathematicians (see [**10, 15**]). As b increases further, we can see

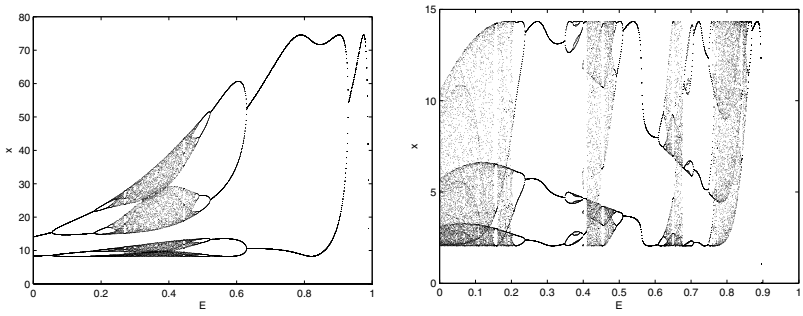

(a) (b)

FIGURE 3. Bifurcation diagrams of equations (3.3) and (3.4) for the population $x(t)$. The effect of parameter E on the dynamical behavior is shown. Parameter values are $k = 1$, $r = 1$, $g = 1.2$, $h = 2$, $d = 0.4$, $\mu = 0.5$, $T_1 = 0.25$, $T_2 = 0.5$. (a) Ricker function, $b = 200$. (b) Beverton-Holt function, $b = 50$, $c = 3$, $n = 10$.

that the population locks into cycles of various periods, which in turn proceeds through its own period-doubling sequences. For the Beverton-Holt function, from Figure 1b we can also observe that the symmetry-breaking (sb) bifurcations occur after the period-doubling bifurcations (symmetry-breaking pitchfork bifurcations, see [**28**], are particularly simple bifurcations which give rise to multiplicity of steady states), which is followed by a cascade of period-halving bifurcation; and then again period-doubling bifurcation occurs, which is also followed by chaos with wide periodic windows.

The bifurcation diagrams of both models reveal another interesting phenomenon. From Figure 2 we notice that if the cycles to the left of a given chaotic window are of period k, then the cycles to the right are period $k + 1$. These so-called "period-adding" sequences have been observed in chemical reactions, see [**15**], and electrical circuits, see [**16**], and have been studied in one-dimensional difference equations [**19**]. "Period-adding" phenomenon is also present in a delay difference equation population model with density-dependent reproduction, see [**4**], and in the density-dependent age-structured model studied by Guckenheimer et al. [**13**].

In Figure 3, we fix another parameter and choose E as a bifurcation parameter. System (3.3) with Ricker function and system (3.4) with Beverton-Holt function both display very complex dynamical behaviors

as E increases. When the parameter E increases to some critical value (for Ricker function, $E = 0.99$; for Beverton-Holt function, $E = 0.89$), the population decreases deeply and eventually goes extinct. In Figure 3a, as the parameter E increases, it exhibits period-doubling bifurcation phenomena leading to chaos, which is eventually followed by a cascade of period-halving bifurcation. In Figure 3b, a sequence of period-doubling bifurcations interchanging with regions of chaos followed by period-halving bifurcations is observed, and it also shows that cascades are oriented in both directions. That is, the periodic orbits are both created and annihilated as E increases. This shows that system (3.4) has the property of antimonotonicity. The phenomenon of "antimonotonicity" was studied by Dawson [**8**].

Similar phenomena can be observed in Figure 4 if we choose μ as the bifurcation parameter. In Figure 4a (for the Ricker function), as the parameter μ increases, there are many chaotic bands, which are followed by a cascade of period-halving bifurcations. In Figure 4b (for the Beverton-Holt function), as the parameter μ increases, system (3.4) experiences a process of chaos $\to$ period-halving cascade $\to$ period-doubling bifurcation $\to$ chaos $\to$ period-halving cascade $\to$ period-doubling bifurcation $\to$ chaos $\to$ period-halving cascade.

All of the above results show that birth pulses, pulse harvesting policy and pulse toxicant input in a polluted environment make the dynamical behavior of system (2.4) more complex.

6. The effects of pulse harvesting time and pulse toxicant input time on the maximum annual-sustainable yield. Many authors are interested in studying the optimal management of renewable resources, which has a direct relationship to sustainable development. From the point of view of ecological managers, it may be desirable to have a unique positive equilibrium which is asymptotically stable, in order to plan harvesting strategies and keep sustainable development of the system. In this section, we will study how the pulse harvesting and pulse toxicant input affect the maximum annual-sustainable yield.

For $b_0 < b < b_c$, the equilibrium $E^*(x^*, c^*, f^*)$ is stable. For this range of b, trajectories of system (2.4) approach the periodic solution $(\tilde{x}(t), \tilde{c}(t), \tilde{f}(t))$ with period 1, that is, periodic solution (4.1) (or (4.2)) of system (2.4) is locally asymptotically stable.

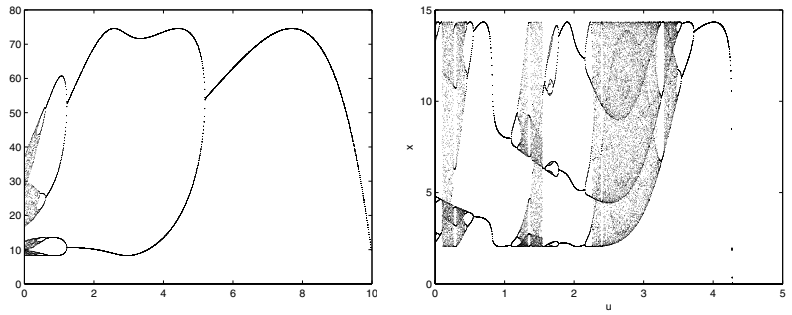

(a) (b)

FIGURE 4. Bifurcation diagrams of equations (3.3) and (3.4) for the population $x(t)$. The effect of parameter μ on the dynamical behavior is shown. Parameter values are $k = 1$, $g = 1.2$, $h = 2$, $r = 1$, $d = 0.4$, $E = 0.5$, $T_1 = 0.25$, $T_2 = 0.5$. (a) Ricker function, $b = 200$. (b) Beverton-Holt function, $b = 50$, $c = 3$, $n = 10$.

Since we only need to consider the annual-sustainable yield in one period, without loss of generality we can choose $m = 0$ and the annual-sustainable yield is

$$X(E) = EX(m + T_2)$$

$$= \begin{cases} Ex^* e^{(krf^*)/(g-h)((1/g)(1-e^{-gT_2})-(1/h)(1-e^{-hT_2}))-(r/g)c^*(1-e^{-gT_2})} \\ \quad + e^{(k\mu r)/(g-h)((1/g)(1-e^{-g(T_2-T_1)})-(1/h)(1-e^{-h(T_2-T_1)}))-dT_2}, \\ \qquad\qquad \text{if } T_1 < T_2, \\ Ex^* e^{(krf^*)/(g-h)((1/g)(1-e^{-gT_2})-(1/h)(1-e^{-hT_2}))-(r/g)c^*(1-e^{-gT_2})-dT_2}, \\ \qquad\qquad \text{if } T_2 < T_1. \end{cases}$$

Our main purpose is to get an $\overline{E}$ such that $X(E)$ reaches its maximum at $\overline{E}$ and study how the maximum annual-sustainable yield $X(\overline{E})$ changes as T_1 or T_2 vary. Numerical analysis implies that there exists a unique E such that $X(E)$ reaches its maximum for each fixed T_1 and T_2 (see Figure 5. For Figure 5a, $X(E)$ reaches its maximum at $\overline{E} = 0.83$; for Figure 5b, $X(E)$ reaches its maximum at $\overline{E} = 0.88$). Also, from Figure 5 and Figure 6 we can observe that the maximum annual-sustainable yield dramatically depends on the pulse harvesting time, and the maximum annual-sustainable harvest yield is largest at $T = 0$ and smallest at $T = 0.8$. This shows that if we harvest immediately

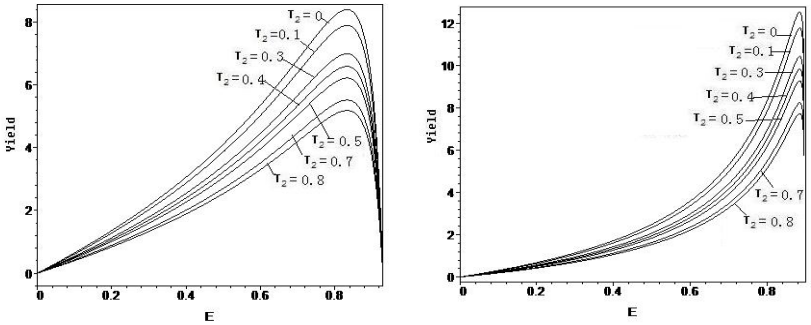

FIGURE 5. Annual-sustainable yield of equations (3.3) and (3.4), showing the relationship between maximum annual-sustainable and the harvesting time. Parameter values are $k = 1$, $g = 1.2$, $h = 2$, $r = 1$, $d = 0.4$, $\mu = 0.5$, $T_1 = 0.5$. (a) Ricker function, $b = 25$. (b) Beverton-Holt function, $b = 50$, $c = 3$, $n = 9$.

after the birth pulse, the largest maximum annual-sustainable harvest yield is obtained; however, if we harvest near the time of the birth pulse, the maximum annual-sustainable yield is smallest. Further, it shows that the maximum annual-sustainable harvest yield is not significantly affected by the time of toxicant input, see Figure 6.

7. Conclusion. In this paper we have investigated the dynamics of a single-species population model with pulse harvesting, pulse toxicant input and birth pulses in a polluted environment. By using the stroboscopic map, we have obtained the complete expression for the 1-period solution and the threshold conditions for their stability. We show the effects of the time of pulse harvesting and the time of pulse toxicant input on the maximum annual-sustainable yield. Our results show that the best time of harvesting is immediately after the birth pulse, and the maximum annual-sustainable yield is not significantly affected by the time of toxicant input. From the viewpoint of biology, the mathematical results are full of biological meanings and can be used to provide reliable foundations for making decisions. Numerical simulation results also show that pulse harvesting, pulse toxicant input and birth pulses make the single-species model in a polluted environment we consider more complex and dominated by periodic and chaotic solutions.

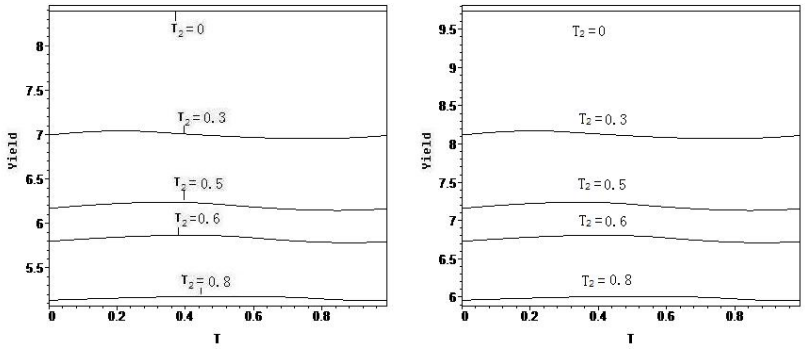

FIGURE 6. The annual-sustainable yield of the equations (3.3) and (3.4), showing the relationship between the maximum annual-sustainable and the toxicant input time T_1. Parameter values are $k = 1$, $g = 1.2$, $h = 2$, $r = 1$, $d = 0.4$, $\mu = 0.5$, $E = 0.83$. From above to below, T_2 is 0, 0.3, 0.5, 0.6, 0.8 respectively. (a) Ricker function, $b = 25$. (b) Beverton-Holt function, $b = 50$, $c = 3$, $n = 9$.

Our results about harvesting and those in [**34**] all conclude that harvest timing is of great importance to annual yield and population persistence, whether it is pulse harvesting or open/closed piecewise continuous-time harvesting. Harvesting too late may overexploit a population risking extinction, with much smaller maximum annual yield as well. Therefore, wider seasonal closures are the best way to adequately protect fish during the spawn season.

REFERENCES

1. Z. Agur, L. Cojocaru, R. Anderson and Y. Danon, *Pulse mass measles vaccination across age cohorts*, Proc. National Acad. Sci. **90** (1993), 11698–11702.

2. L.H.R. Alvarez, *Optimal harvesting under stochastic fluctuations and critical depensation*, Math. Biosci. **152** (1998), 63–85.

3. D. Bainov and P. Simeonov, *Impulsive differential equations: periodic solutions and applications*, Pitman Monographs Surveys Pure Appl. Math. **66** (1993).

4. L.W. Botsford, *Further analysis of Clark's delayed recruitment model*, Bull. Math. Biol. **54** (1992), 275–293.

5. G. Caughley, *Analysis of vertebrate populations*, John Wiley & Sons, New York, 1977.

6. C.W. Clark, *Mathematical Bioeconomics: The Optimal Management of Renewable Resources*, 2nd ed., Wiley, New York, 1990.

7. A. D' Onofrio, *Stability properties of pulse vaccination strategy in* SEIR *epidemic model*, Math. Biosci. **179** (2002), 57–72.

8. S.P. Dawson, C. Grebogi and J.A. Yorke, *Antimonotononicity: Inevitable reversals of period-doubling cascades*, Phys. Lett. **162**, (1992), 249–254.

9. B. Dubey, *Modelling the interaction of two biological species in a polluted environment*, J. Math. Anal. Appl. **246** (2000), 58–79.

10. J.P. Eckmann, *Routes to chaos with special emphasis on period doubling*, in *Chaotic behaviour of deterministic systems*, G. Iooss, et al., eds., Elsevier, North-Holland, 1983.

11. H.I. Freedman and T.B. Shukla, *Models for the effect of toxicant in single-species and predator-prey systems*, J. Math. Biol. **30** (1991), 15–30.

12. E. Funasaki and M. Kot, *Invasion and chaos in a periodically pulsed mass-action chemostat*, Theoret. Population Biol. **44** (1993), 203–224.

13. J. Guckenheimer, G. Oster and A. Ipaktchi, *The dynamics of density dependent population models*, J. Math. Biol. **4** (1997), 101–147.

14. T.G. Hallam and Z. Ma, *Persistence in population models with demographic fluctuations*, J. Math. Biol. **24**, (1986), 327–339.

15. M.J.B. Hauser, L.F. Olsen, T.V. Bronnikova, and W.M. Schaffer, *Routes to chaos in the peroxidase-oxidase reaction: Period-doubling and period-adding*, J. Phys. **101** (1997), 5075–5083.

16. Y.F. Hung, T.C. Yen and J.L. Chern, *Observation of period-adding in an optogalvanic circuit*, Phys. Lett. **199** (1995), 70–74.

17. E.L. Johnston and M.J. Keough, *Field assessment of effects of timing and frequency of copper pulses on settlement of sessile marine invertebrates*, Marine Biology **137** (2000), 1017–1029.

18. Emma L. Johnston, Michael J. Keough and Pei-Yuan Qian, *Maintenance of species dominance through pulse disturbances to a sessile marine invertebrate assemblage in Port Shelter, Hong Kong*, MEPS **226** (2002), 103–114.

19. A.L. Kawczynski and M. Misiurewicz, *Period adding phenomenon in* 1D *return maps*, Z. Physik. Chem. **271** (1990), 1037–1046.

20. A. Lakmeche and O. Arino, *Bifurcation of non trivial periodic solutions of impulsive differential equations arising chemotherapeutic treatment*, Dynamics of Continuous, Discrete Impulsive Syst. **7** (2000), 165–287.

21. V. Lakshmikantham, D. Bainov and P. Simeonov, *Theory of impulsive differential equations*, World Scientific, Singapore, 1989.

22. B. Liu and L.S. Chen, *Dynamic complexities in Lotka-Volterra predator-prey system concerning impulsive control strategy*, Internat. J. Bifurcation Chaos **15** (2005), 517–531.

23. ———, *Complex dynamics of Holling type* II *Lotka-Volterra predator-prey system with impulsive perturbations on the predator*, Chaos, Solitons Fractals **16** (2003), 311–320.

24. B. Liu, L.S. Chen and Y.J. Zhang, *The effects of impulsive toxicant input on a population in a polluted environment*, J. Biol. Syst. **11** (2003), 265–274.

25. B. Liu, Y.J. Zhang and L.S. Chen, *Dynamic complexities of a Holling* I *predator-prey model concerning periodic biological and chemical control*, Chaos, Solitons Fractals **22** (2004), 123–134.

26. ———, *The dynamical behaviors of a Lotka-Volterra predator-prey model concerning integrated pest management*, Nonlinear Analysis: Real World Applications **6** (2005), 227–243.

27. R.M. May and G.F. Oster, *Bifurcations and dynamic complexity in simple ecological models*, Amer. Natur. **110** (1976), 573–599.

28. J.C. Paneyya, *A mathematical model of periodically pulsed chemotherapy: Tumor recurrence and metastasis in a competition environment*, Bulletin Math. Biol. **58** (1996), 425–447.

29. S. Riidiger, *Practical bifurcation and stability analysis from equilibrium to chaos*, Springer-Verlag, New York, 1994.

30. M.G. Roberts and R.R. Kao, *The dynamics of an infectious disease in a population with birth pulse*, Math. Biosci. **149** (1998), 23–36.

31. B. Shulgin, L. Stone and Z. Agur, *Theoretical examination of pulse vaccination policy in the SIR epidemic model*, Mathematical Computer Modelling **31** (2000), 207–215.

32. S.Y. Tang and L.S. Chen, *The effect of seasonal harvesting on stage-structured population models*, J. Math. Biol. **48** (2004), 357–374.

33. M. Tapan and R. Santanu, *Optimal exploitation of renewable resources under uncertainty and the extinction of species*, Economic Theory **28** (2006), 1–23.

34. C. Xu, M.S. Boyce and D.J. Daley, *Harvesting in seasonal environments*, J. Math. Biol. **50** (2005), 663–682.

Applied Mathematics, Dalian University of Technology, Dalian 116024, Liaoning, P.R. China and Department of Mathematics, Anshan Normal University, Anshan 114007, Liaoning, P.R. China
Email address: taofm@yeah.net

Department of Mathematics, Anshan Normal University, Anshan 114007, Liaoning, P.R. China
Email address: liubing529@126.com